© 2018. Published by The Company of Biologists Ltd | Journal of Cell Science (2018) 131, jcs213017. doi:10.1242/jcs.213017

RESEARCH ARTICLE

Soluble α-synuclein facilitates priming and fusion by releasing Ca^{2+} from the thapsigargin-sensitive Ca^{2+} pool in PC12 cells

Chien-Chang Huang[1,2], Tai-Yu Chiu[2], Tzu-Ying Lee[2], Hsin-Jui Hsieh[2], Chung-Chih Lin[1,2,3,*] and Lung-Sen Kao[1,2,*]

ABSTRACT

α-Synuclein is associated with Parkinson's disease, and is mainly localized in presynaptic terminals and regulates exocytosis, but its physiological roles remain controversial. Here, we studied the effects of soluble and aggregated α-synuclein on exocytosis, and explored the molecular mechanism by which α-synuclein interacts with regulatory proteins, including Rab3A, Munc13-1 (also known as Unc13a) and Munc18-1 (also known as STXBP1), in order to regulate exocytosis. Through fluorescence recovery after photobleaching experiments, overexpressed α-synuclein in PC12 cells was found to be in a monomeric form, which promotes exocytosis. In contrast, aggregated α-synuclein induced by lactacystin treatment inhibits exocytosis. Our results show that α-synuclein is involved in vesicle priming and fusion. α-Synuclein and phorbol 12-myristate 13-acetate (PMA), which is known to enhance vesicle priming mediated by Rab3A, Munc13-1 and Munc18-1, act on the same population of vesicles, but regulate priming independently. Furthermore, the results show a novel effects of α-synuclein on mobilizing Ca^{2+} release from thapsigargin-sensitive Ca^{2+} pools to enhance the ATP-induced $[Ca^{2+}]_i$ increase, which enhances vesicle fusion. Our results provide a detailed understanding of the action of α-synuclein during the final steps of exocytosis.

KEY WORDS: α-Synuclein, Rab3A, Exocytosis, Priming, Dilation of fusion pore, TG-sensitive pools

INTRODUCTION

α-Synuclein is a small soluble protein that is highly abundant in nerve terminals (Maroteaux et al., 1988). It is the major component of Lewy bodies and is present in the polymerized fibrils found in the brains of patients who suffer from Parkinson's disease (Spillantini et al., 1998). The familial A30P and A53T mutations, and the expression of the abnormal α-synuclein, have been suggested to play key roles in the neurodegenerative process associated with Parkinson's disease (Narhi et al., 1999). α-Synuclein has also been shown to associate with the plasma membrane and is found as a soluble protein in human and mouse brain extracts (Fortin et al., 2004; Kahle et al., 2000) and in rat hippocampal neurons (Fortin et al., 2005). Overexpression of human α-synuclein leads to abnormal aggregation and neuronal degeneration both at the cellular level (Outeiro et al., 2008) and in a mouse model (Masliah et al., 2000). Studies on transgenic mice overexpressing α-synuclein, show that α-synuclein has at least three distinct subcellular forms in presynaptic terminals. These consist of unbound soluble protein, proteins bound to presynaptic vesicles and proteins in the form of microaggregates (Spinelli et al., 2014).

Several lines of evidence have shown that α-synuclein is involved in the regulation of exocytosis. Firstly, α-synuclein is mainly localized within the presynaptic terminals and has been reported to regulate the size of the presynaptic vesicular pool, vesicular turnover, synaptic plasticity and the assembly of the soluble NSF attachment protein receptor (SNARE) complex (Abeliovich et al., 2000; Cabin et al., 2002; Chandra et al., 2005; Larsen et al., 2006; Murphy et al., 2000). Secondly, α-synuclein is able to rescue neurodegeneration caused by knockout of the synaptic co-chaperone protein cysteine-string protein-α (CSPα; also known as DNAJC5) (Chandra et al., 2005). Thirdly, α-synuclein has been shown to perturb Ca^{2+} homeostasis in SH-SY5Y cells (Hettiarachchi et al., 2009). Ca^{2+} plays important roles in the regulation of exocytosis, including the activation of phospholipase C and the assembly of the SNARE complex (Giraudo et al., 2006). According to previous biochemical investigations, α-synuclein directly interacts with several synaptic proteins, including Rab3A, rabphilin, septin-4 and synapsin 1 (Dalfó et al., 2004a; Ihara et al., 2007; Nemani et al., 2010). However, it remains unclear as to how α-synuclein interacts with molecules that are involved in exocytotic process within living cells.

It has been shown that Rab3A associates with α-synuclein in Lewy bodies (Dalfó et al., 2004a). Rab3A is a small G-protein of Rab family that is involved in the late steps of exocytosis. Rab3A acts as a gate keeper and plays multiple roles in the secretory process, including in docking, priming and fusion (Dulubova et al., 2005; Huang et al., 2011; Leenders et al., 2001; Lin et al., 2007; Wang et al., 2008). It has been shown that α-synuclein is present in the homogenate obtained from the entorhinal cortex from Lewy body disease patients and can be pulled down with Rab3A by immunoprecipitation (Dalfó et al., 2004a,b). We have previously found that the rate of Rab3A dissociation is involved in regulating fusion pore dilation and that Rab3A also involved in modulating Munc13-1 (also known as Unc13a)- and Munc18-1 (also known as STXBP1)-dependent vesicle priming (Huang et al., 2011; Lin et al., 2007).

In this study, we focus on the effects of soluble α-synuclein and its aggregates on exocytosis, and explored the molecular mechanism by which α-synuclein interacts with regulatory proteins, including Rab3A, Munc13-1 and Munc18-1, to regulate exocytosis. This was carried out by using total internal reflection fluorescence (TIRF) microscopy to examine the process of exocytosis in living PC12 cells. Our results suggest that α-synuclein acts at multiple steps during exocytosis including

[1]Brain Research Center, National Yang-Ming University, Taipei 112, Taiwan, Republic of China. [2]Department of Life Sciences and Institute of Genome Sciences, National Yang-Ming University, Taipei 112, Taiwan, Republic of China. [3]Biophotonics Interdisciplinary Research Center, National Yang-Ming University, Taipei 112, Taiwan, Republic of China.

*Authors for correspondence (lskao@ym.edu.tw; cclin2@ym.edu.tw)

C.-C.H., 0000-0001-8089-251X; T.-Y.L., 0000-0001-6275-0550; C.-C.L., 0000-0002-3390-882X; L.-S.K., 0000-0001-6712-8306

Received 28 November 2017; Accepted 12 October 2018

Journal of Cell Science (2018) 131, jcs213017. doi:10.1242/jcs.213017

priming and fusion. α-Synuclein and the Rab3A–Munc13-1–Munc18-1 pathway regulate the priming and fusion of the same population of vesicles using different pathways. Our studies also reveal a novel role of α-synuclein, which affects fusion via an enhancement of Ca^{2+} release from thapsigargin-sensitive Ca^{2+} pools.

RESULTS

Effects of α-synuclein on the late stages of exocytosis

We first examined the effects of α-synuclein on ATP-induced exocytosis of NPY–EGFP-labeled secretory vesicles in PC12 cells. ATP was used to stimulate exocytosis because it stimulates a large and reliable Ca^{2+}-dependent secretory response in PC12 cells (Lin et al., 2007). TIRF microscopy was used to monitor the exocytosis of the vesicles. The same ATP stimulation and TIRF microscopy was used to study the exocytotic machinery (Lin et al., 2007; Huang et al., 2011). In this study, the role of α-synuclein in exocytosis was studied under similar experimental conditions, so that the results can be compared directly.

The patterns of change in fluorescence intensity of the vesicles during exocytosis can be divided into three types; these reflect the dilation rate of the fusion pore (Fig. 1A; Huang et al., 2011; Lin et al., 2007). During the type 1 changes, the vesicles show a transient increase in fluorescence and then the fluorescence decreases gradually but does not return to its basal level. This is likely to be the result of a brief opening of the fusion pore and then the re-acidification of the vesicle, which lowers the fluorescence of the NPY-tagged EGFP, a pH-sensitive protein. Only a few exocytotic events occurred as a type 1 event under the experimental conditions used in this study. The type 2 pattern shows a transient increase in fluorescence, then the fluorescence disperses and decreases rapidly back to its background value. This represents the typical exocytosis of NPY–EGFP-labeled vesicles in which the NPY–EGFP is released and then diffuses into the extracellular milieu. We have previously shown that extracellular Bromophenol Blue, which quenches the fluorescence of NPY–EGFP, is able to inhibit the fluorescence transients that occurs during both type 1 and type 2 secretion. Furthermore, when using the proton pump inhibitor bafilomycin A1 to neutralize the pH of the intracellular vesicles, the fluorescent transient of NPY–EGFP disappears during fusion pore opening. These results support the idea that the fluorescence transients are due to fusion pore opening rather than the vesicle approaching the evanescent field (Huang et al., 2011). The type 3 pattern shows an abrupt decrease in fluorescence to the background level without any transient increase. This represents a fast opening of the fusion pore accompanied by fluorescence diffusion and dispersion, with this process being too fast to be caught by the imaging system (Huang et al., 2011).

In the control PC12 cells, phorbol 12-myristate 13-acetate (PMA) enhanced ATP-induced exocytosis by 1.68 fold (Fig. 1B), which can be accounted for by the increase in the percentage of type 3 exocytosis (Fig. 1C). In α-synuclein-overexpressing PC12 cells, ATP-induced exocytosis was found to be enhanced by 1.63 fold, and PMA pretreatment, which increases vesicle priming, did not cause any further increase. In α-synuclein-overexpressing cells, the percentage of type 3 exocytosis was increased to a higher level, but the total exocytotic activity was similar to that caused by PMA treatment alone (Fig. 1C). To confirm that the three types of fluorescence changes are due to fusion pore opening, experiments are also performed using NPY–pHluorin. The results were similar to those obtained with NPY–EGFP (Fig. S1). These findings support the hypothesis that α-synuclein is involved in the priming step of

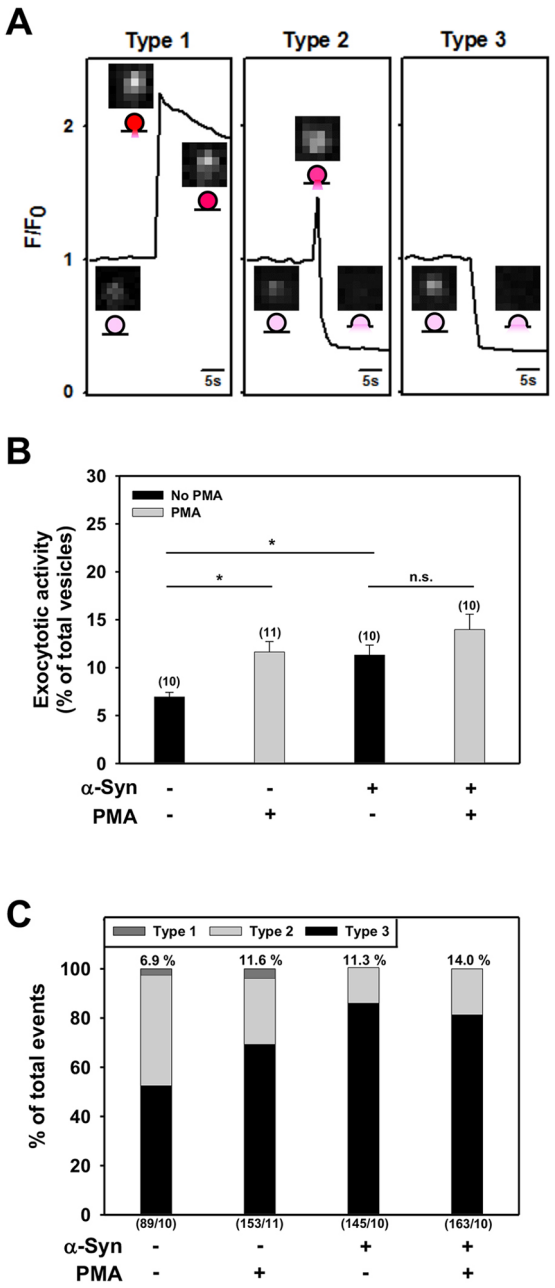

Fig. 1. α-Synuclein enhances the late steps of exocytosis. PC12 cells were co-transfected with pECFP-C1 or pECFP-α-synuclein (α-Syn) and pNPY-EGFP to monitor vesicle secretion. The transfected cells were pre-treated with 100 nM PMA for 10 min. The fluorescence changes in the NPY–EGFP-labeled vesicles upon ATP stimulation for 10 s were monitored by TIRF microscopy and analyzed as described in the Materials and Methods. (A) The ATP-triggered fluorescence changes of the NPY–EGFP-labeled vesicles can be divided into three patterns. Representative images of single vesicles show the different patterns of fluorescence changes. Traces under each image show the fluorescence intensity of the individual pixels across the center of the vesicle. (B) Effects of α-synuclein on secretory activity. The secretory activity is shown as a percentage of the total NPY–EGFP-labeled vesicles in the evanescent field released in 2 min under various conditions. (C) The distributions of the three patterns of NPY–EGFP release are shown as a percentage of total exocytotic events. The number shown above each column represents the percentage of vesicles released in 2 min and is based on the data shown in B. The number of cells and total number of exocytotic events examined are indicated in the parenthesis under each column. The data shown are the mean±s.e.m. from the number of cells indicated and were obtained from at least three independent transfections. *P<0.05; n.s., not significant vs control without PMA (Student's t-test).

Journal of Cell Science (2018) 131, jcs213017. doi:10.1242/jcs.213017

exocytosis and also accelerates the dilation of the fusion pore. Vesicles in the evanescent field were counted as 'morphologically docked' vesicles (Huang et al., 2011; Zenisek et al., 2000). The number of docked vesicles was not affected by overexpression of α-synuclein (Table S1). This finding shows that α-synuclein is not involved in the docking of vesicles.

Aggregation of α-synuclein inhibits exocytosis

To study the effect of aggregated α-synuclein on exocytosis, a proteasome inhibitor, lactacystin was used to induce the aggregation of α-synuclein (Rideout et al., 2001). Note, that we did try to overexpress α-synuclein A53T mutant and double mutant (A30T/A53T) in PC12 cells, but no aggregation of either mutant was found (data not shown). After lactacystin treatment for 24 h, α-synuclein was found to be present in the aggregated form, while ECFP, as a control molecule, was homogeneously distributed throughout the cytosol (Fig. 2A, see also Fig. 3). After lactacystin treatment, ATP-induced secretion was significantly inhibited, by 60%, in cells that were overexpressing α-synuclein (Fig. 2B). ATP-induced secretion from control cells was not affected by the lactacystin treatment. Furthermore, the enhancement of type 3 secretion upon overexpression of α-synuclein was not affected by lactacystin treatment (Fig. 2C). Taken together with our other results (see later; Figs 6D, 7D), these findings suggest that aggregated α-synuclein perturbs vesicle priming, but does not affect fusion pore dilation.

Overexpressed α-synuclein protein is soluble

To confirm that lactacystin induced the aggregation of α-synuclein in PC12 cells under our experimental conditions, fluorescence recovery after photobleaching (FRAP) was measured. Representative FRAP images and the distribution of recovery half-life ($t_{1/2}$) of a number of different proteins are presented in Fig. 3. ECFP and EGFP were used as markers for soluble proteins. EYFP–actin within the areas where stress fibers were present was used as a marker for aggregated proteins. Trimeric EGFP ($EGFP_3$) was used to simulate the ECFP–α-synuclein dimer because they have similar molecular masses. The $t_{1/2}$ value of EYFP–actin was much longer than the $t_{1/2}$ values of the other proteins, and ranged from 2 s to 22 s with an average of 8.25 s (n=27). By way of contrast, the $t_{1/2}$ of overexpressed ECFP–α-synuclein was between 0.2 s and 1 s with an average of 0.51 s (n=28), which is significantly smaller than that of $EGFP_3$ (range, 0.8 s to 2 s; average, 1.1 s; n=22) and longer than EGFP (range, 0.2 s to 0.8 s; average, 0.35 s; n=17) and ECFP (range, 0.2 s to 1.7 s; average, 0.37 s; n=31). The $t_{1/2}$ of the aggregated ECFP–α-synuclein was found to be between 4 s and 24 s, with an average of 10.42 s (n=34). Based on the $t_{1/2}$, the diffusion coefficient of aggregated ECFP–α-synuclein is calculated to be 0.1–0.2 $\mu m^2/s$ (Reits and Neefjes, 2001) and the molecular mass is estimated to be >1000 kDa (Kumar et al., 2010). These findings indicate that the overexpressed ECFP–α-synuclein protein is present as the soluble form in PC12 cells and become aggregated after lactacystin treatment. It should be noted that the endogenous level of α-synuclein in PC12 cells is low (Fig. S2) and lactacystin was found to have no effect on secretion in the control cells when there was no overexpression of α-synuclein (Fig. 2B).

Overexpression of α-synuclein affects the late steps of exocytosis and this is independent of the dissociation of Rab3A

α-Synuclein has been shown to co-immunoprecipitate with Rab3A (Chen et al., 2013; Dalfó et al., 2004a). Rab3A is known to act as a

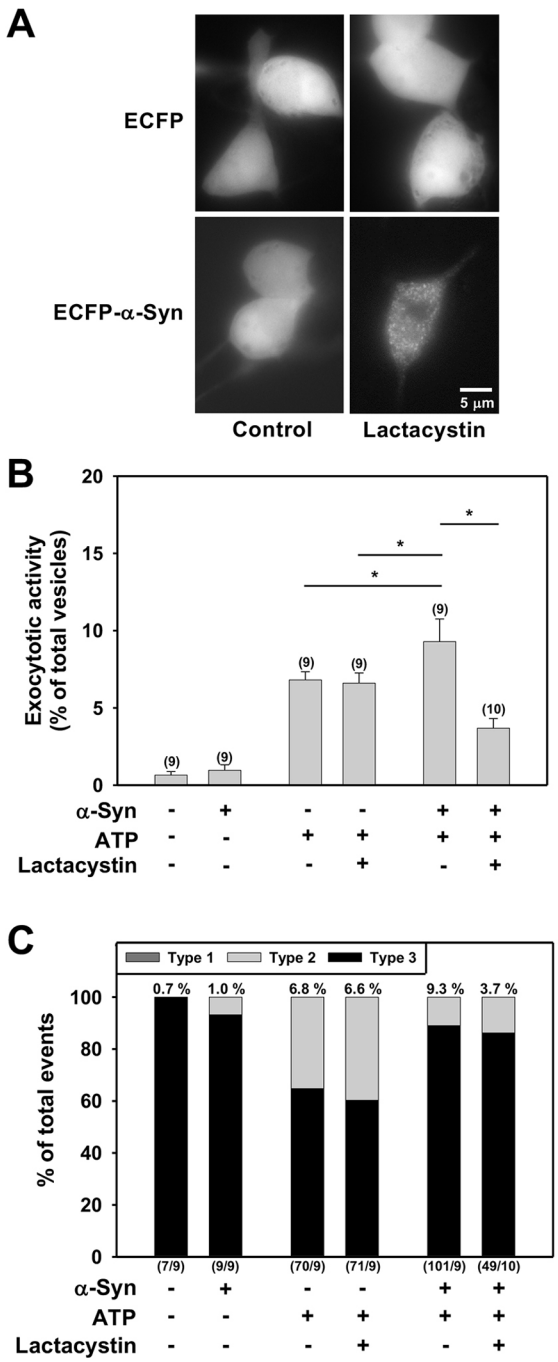

Fig. 2. Effects of aggregated α-synuclein on the late steps of exocytosis. PC12 cells were co-transfected with pNPY-EGFP, and pECFP-C1 (ECFP) or pECFP-α-synuclein (ECFP–α-Syn). The transfected cells were pre-treated with 5 μM lactacystin for 24 h. Fluorescence changes of the NPY–EGFP-labeled vesicles upon ATP stimulation were monitored by TIRF microscopy to assess vesicle secretion. (A) Representative images of the ECFP fluorescence after lactacystin treatment. (B) Effects of lactacystin on exocytotic activity. Exocytosis was triggered by ATP stimulation for 10 s and monitored by TIRF microscopy. Results shown are the percentages of total NPY–EGFP-labeled vesicles in the evanescent field secreted in 2 min. The data shown are mean ±s.e.m. from the number of cells indicated in the parenthesis and were obtained from three independent transfections. *P<0.05 (Student's t-test). (C) The distributions of the three patterns of NPY–EGFP release are shown as a percentage of total exocytosis events. The number shown above each column represents the percentage of vesicles released in 2 min based on the data shown in B. The number in parenthesis below each column represents ratios of the number of vesicles released to numbers of the cells.

Journal of Cell Science (2018) 131, jcs213017. doi:10.1242/jcs.213017

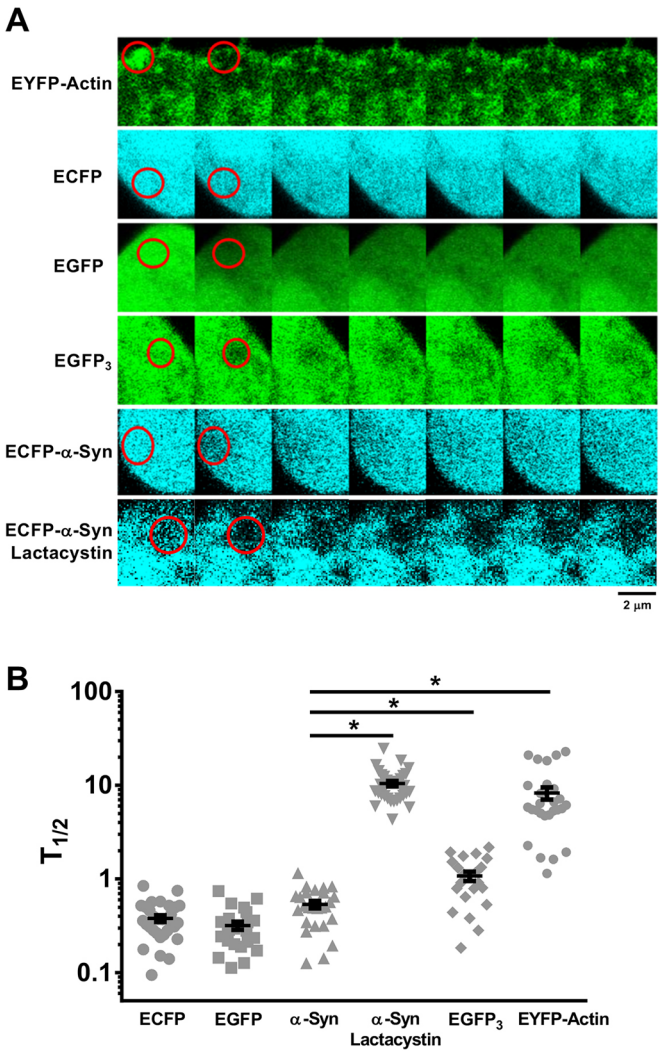

Fig. 3. FRAP results confirm the presence of the monomeric form of overexpressed α-synuclein in PC12 cells. PC12 cells were transfected with pECFP-C1 (ECFP), pEGFP-C1 (EGFP), pEGFP-trimer ($EGFP_3$), pEYFP-Actin (EYFP-Actin), pECFP-α-synuclein (ECFP-α-syn), or with pECFP-α-synuclein and treated with lactacystin (ECFP-α-syn Lactacystin) as indicated. (A) Representative FRAP images of the different proteins are shown. (B) Distributions of recovery half-life ($t_{1/2}$) of the different proteins. Data shown are the mean±s.e.m., and were obtained from at least three independent transfections. *P<0.05 (Student's t-test; n=17–34).

gatekeeper for exocytosis, and it has been found to play multiple roles in the regulation of exocytosis, including vesicle priming and the opening of fusion pore (Huang et al., 2011; Lin et al., 2007). To study whether Rab3A is involved in the enhancement of exocytosis by α-synuclein, α-synuclein was co-expressed with EGFP–Rab3A in PC12 cells. Upon ATP stimulation, the fluorescence of EGFP–Rab3A dispersed into a larger area before it disappeared (Fig. 4A). This represents the fact that the Rab3A dissociates from vesicles and diffuses away from the evanescence field, and such phenomena are correlated with the occurrence of exocytosis (Lin et al., 2007). In α-synuclein-overexpressing cells, neither the rate of Rab3A dissociation from the vesicles nor the rate of occurrence of Rab3A dissociation events, was affected (Fig. 4A). Thus, it would seem that Rab3A is not involved in the enhancement of exocytosis by α-synuclein.

In addition to the above, the effects of geldanamycin (GA), an inhibitor of the dissociation of Rab3A and heat shock protein 90 (Hsp90) family proteins (Sakisaka et al., 2002), were examined. Both Rab3A dissociation and the occurrence of exocytosis were decreased and delayed as the concentration of GA was increased (Fig. 4B), this could not be rescued by overexpression of α-synuclein (Fig. 4B). Furthermore, GA did not affect the distribution pattern during vesicle release; the increased number of type 3 events brought about by overexpression of α-synuclein during exocytosis remained when GA was present (Fig. 4C). These findings support that hypothesis that the effects of α-synuclein on regulating exocytosis is Rab3A independent.

α-Synuclein competes with the Rab3A-dependent pathway for the priming of the same vesicle population

To further elucidate the relationship between Rab3A and α-synuclein, Rab3A and its mutants were co-expressed with α-synuclein in PC12 cells. RT-PCR analysis shows that overexpression of α-synuclein does not affect the expression of Rab3A and its mutants (Fig. S3). The results showed that Rab3A and its mutants affected ATP-induced exocytotic activity with similar trends to that found in the control cells and in α-synuclein-overexpressing cells (Fig. 5A versus B, black bars). In Rab3A-overexpressing cells or cells expressing the constitutively active mutant Rab3A-Q81L, ATP-induced exocytotic activity was inhibited in both the control cells and in α-synuclein-overexpressing cells. In cells expressing the dominant-active mutant Rab3A-T36N and Rab3A-knockdown cells, ATP-stimulated exocytosis was increased. After PMA treatment, which increases vesicle priming, the exocytosis that occurred in cells overexpressing Rab3A-T36N or Rab3A-knockdown cells was dramatically increased, by ∼2 fold (Fig. 5A, gray bars). However, this enhancement by PMA was significantly reduced by overexpression of α-synuclein (Fig. 5B, gray bars). Further analysis of the patterns of exocytosis shows that ATP-induced type 3 exocytosis was enhanced by overexpression of α-synuclein; however, this was not significantly affected upon overexpression of Rab3A or its mutants, or when there was knockdown of Rab3A (Fig. 5C; Huang et al., 2011). These results show that Rab3A is able to regulate the occurrence of exocytosis and continues to act as a gate keeper even when α-synuclein is overexpressed. Rab3A and α-synuclein would therefore seem to act on the same population of vesicles via different pathways during the regulation of exocytosis, and when this occurs overexpression of α-synuclein results in a reduction in the effects of PMA.

The molecular mechanism of α-synuclein during vesicle priming

PMA-enhanced vesicle priming is known to be mediated by Rab3A, Munc13-1 and Munc18-1 (Huang et al., 2011; Rhee et al., 2002). We therefore next studied whether Munc13-1 and Munc18-1 are involved in the effects of α-synuclein on secretion. RT-PCR analysis showed that overexpression of α-synuclein does not affect the expression of Munc13-1 and Munc18-1 (Fig. S4). α-Synuclein-enhanced exocytosis was found to be inhibited by overexpression of Munc13-1 (Fig. 6A). We have previously found that a combination of overexpression of Munc13-1 and a knockdown of Rab3A almost completely inhibited exocytosis (Huang et al., 2011). This inhibition of exocytosis and the effects of PMA were rescued by α-synuclein expression (Fig. 6A).

Overexpression of Munc18-1 also reduced α-synuclein-enhanced exocytosis to the level of the control cells, but had no significant effect on PMA-induced exocytosis (Fig. 6B). Overexpression of the dominant-negative syntaxin 1A-binding deficient Munc18-1 mutant R39C (Fisher et al., 2001), inhibited ATP-induced secretion and

Journal of Cell Science (2018) 131, jcs213017. doi:10.1242/jcs.213017

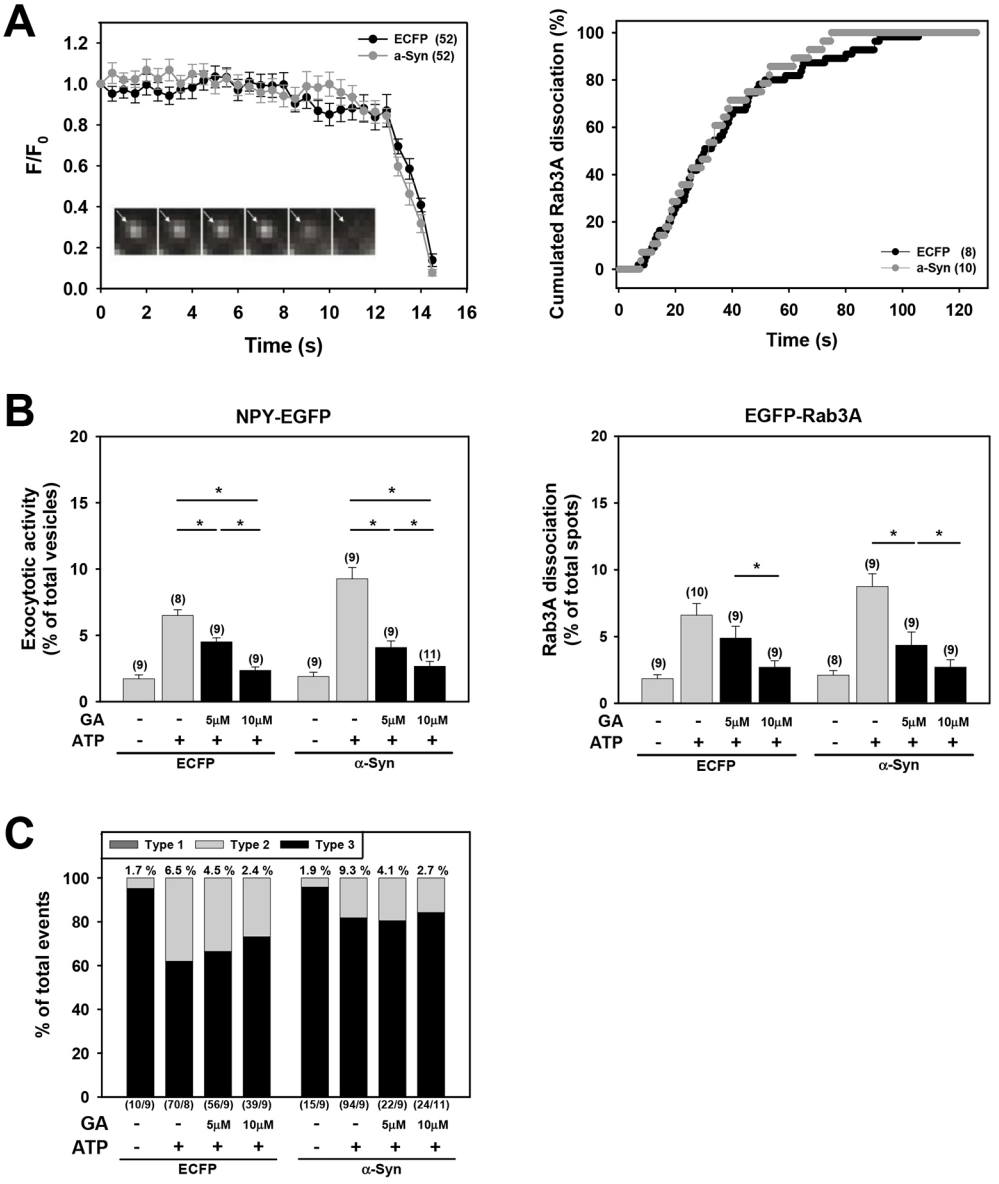

Fig. 4. α-Synuclein has no effect on Rab3A dissociation and Rab3A-regulated fusion pore dilation. (A) PC12 cells were co-transfected with pEGFP-Rab3A and pECFP-C1 (black circles), or ECFP–α-synuclein (gray circles). The transfected cells were stimulated by 100 µM ATP. Dissociation of Rab3A from vesicles was monitored by TIRF microscopy. Left panel: time-lapse images of a representative Rab3A dissociation event are shown in the inset (arrows highlight the Rab3A-associated vesicles). All events were synchronized at the time frame before dissociation, and the mean F/F_0 for these events is plotted. Right panel, cumulative Rab3A dissociation events from the time of ATP stimulation (time 0). (B) NPY–EGFP- or EGFP–Rab3A-overexpressing PC12 cells were pretreated with various concentrations of GA as indicated, and then stimulated with 100 µM ATP to trigger Rab3A dissociation and exocytosis. The exocytotic activities and the rates of Rab3A dissociation are shown as percentages of the total NPY–EGFP-labeled vesicles (left panel) and EGFP–Rab3A-associated vesicles (right panel) in the evanescent field that were secreted in 2 min. *P<0.05 (Student's t-test; n=8–11). (C) The distribution of the three patterns of NPY–EGFP release are shown as a percentage of the total exocytotic events. The number shown above each column represents the percentage of vesicles released in 2 min and is based on the data shown in B. The data shown are the mean±s.e.m. from numbers of total released events or the cells as indicated in the parenthesis and were obtained from at least three independent transfections.

abolished the effects of PMA. Again, the PMA-enhanced exocytosis was able to be rescued by α-synuclein expression.

The above results show that overexpression of α-synuclein affects the PMA-activated Rab3A–Munc13-1–Munc18-1 pathway, to further clarify whether α-synuclein and PMA act on the same pathway, a constitutively active truncated Munc13-1 mutant (comprising amino acids 1–128; herein denoted 128-Munc13-1; Lu et al., 2006), was co-expressed with α-synuclein and with Munc18-1 or Munc18-1-R39C (Fig. 6C). Overexpression of 128-Munc13-1 enhanced ATP-induced secretion in both the control and PMA-treated cells. Similar levels of exocytotic activity were observed in cells co-expressing Munc18-1 or Munc18-1-R39C, which supports the dominant role of 128-Munc13-1. However, when α-synuclein was co-expressed, the enhancement effects of 128-Munc13-1 on PMA-treated cells were abolished. Thus, these results are in accordance with the hypothesis that α-synuclein and PMA regulate priming of the same population of vesicles via different regulation steps that involve Rab3A, Munc13-1 and Munc18-1.

Finally, aggregated α-synuclein inhibited the dominant role of 128-Munc13-1 (Fig. 6D). The aggregated α-synuclein would seem to inhibit vesicle priming and bring about an inhibition of vesicle secretion.

Soluble α-synuclein increases ATP-evoked Ca^{2+} transients that affect exocytosis

To investigate whether the effects of overexpressed soluble and aggregated α-synuclein on vesicle secretion are mediated via changes in the ATP-induced Ca^{2+} response, fura-2-AM was used to monitor the changes of cytosolic Ca^{2+} concentration ($[Ca^{2+}]_i$). Both soluble and aggregated α-synuclein enhanced the ATP-evoked $[Ca^{2+}]_i$ increase, with the peak level of the Ca^{2+} transients being increased by 49% and 43% in the control and lactacystin-treated cells, respectively (Fig. 7A). In cells treated with lactacystin, the basal $[Ca^{2+}]_i$ was increased. The ATP-stimulated cytosolic Ca^{2+} level did not return to the basal level in these cells. When thapsigargin (TG), an inhibitor of the endoplasmic reticulum (ER) Ca^{2+}-ATPase, was used to deplete the ER Ca^{2+} pools, the enhancement effect of α-synuclein overexpression on both the Ca^{2+} transients and exocytotic activity were abolished (Fig. 7B,C). Interestingly, the rate of exocytosis in cells overexpressing soluble α-synuclein is delayed by TG (the delay

Journal of Cell Science (2018) 131, jcs213017. doi:10.1242/jcs.213017

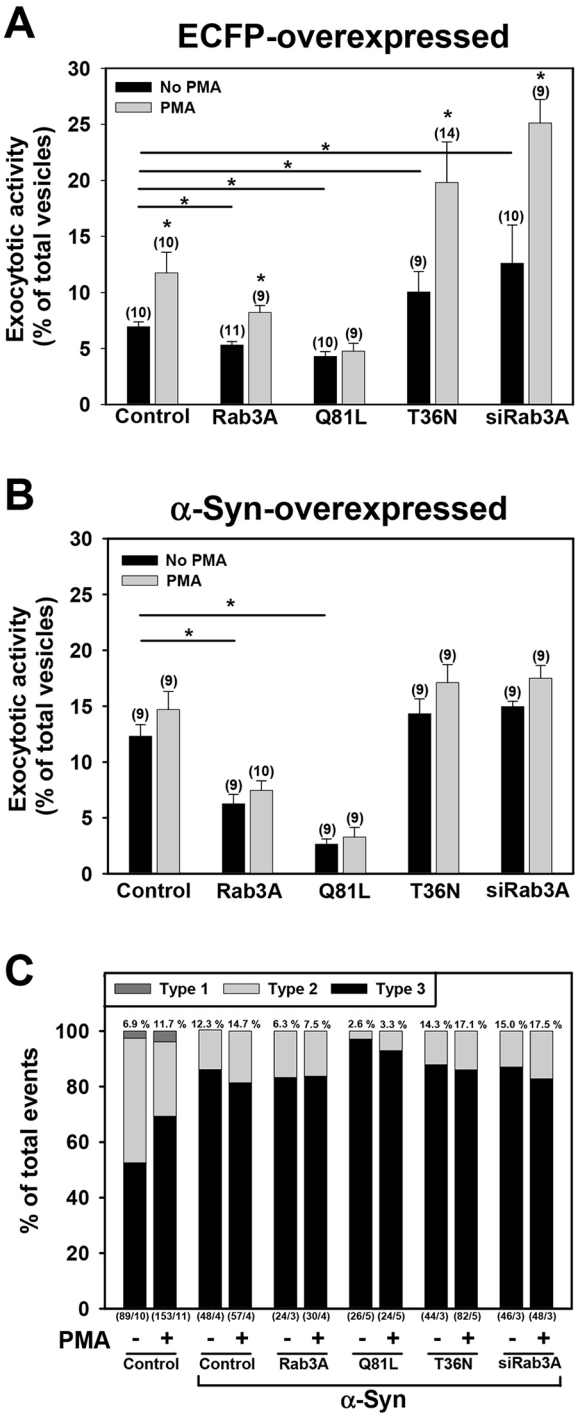

Fig. 5. Effects of α-synuclein on Rab3A-regulated exocytosis. PC12 cells were co-transfected with pNPY-EGFP, pECFP-C1 (A) or pECFP-α-synuclein (B), and pECFP-C1 (Control), pECFP-Rab3A (Rab3A), pECFP-Rab3A-Q81L (Q81L), pECFP-Rab3A-T36N (T36N) or pSilencer-Rab3A (siRab3A) as indicated. The transfected cells were pre-treated with control buffer or 100 nM PMA for 10 min. Fluorescence changes of the NPY–EGFP-labeled vesicles upon ATP stimulation were monitored by TIRF microscopy. The exocytotic activities of cells overexpressing ECFP (A) and α-synuclein (B) are shown as the percentages of the total NPY–EGFP-labeled vesicles in the evanescent field that were secreted in 2 min. (C) The distributions of the three types of NPY–EGFP release pattern in cells overexpressing ECFP (A) and α-synuclein (B) were analyzed, and are shown as a percentage of total exocytotic events. The data shown are mean ±s.e.m. from the ratios of numbers of vesicles released to numbers of cells indicated in the parenthesis and were obtained from at least three independent transfections. *P<0.05 vs control without PMA (Student's t-test; n=3–11).

in reaching the half maximal release was ∼10 s; Fig. 7C, right panel). These findings show that soluble α-synuclein is able to enhance ATP-evoked exocytosis via its effects on Ca^{2+} release from the TG-sensitive Ca^{2+} pools.

The above results show that the enhancement of secretion mediated by PMA was abolished in α-synuclein-overexpressing cells (Figs 5 and 6). To further elucidate which step in exocytosis is affected by the actions of α-synuclein on $[Ca^{2+}]_i$, the RIM-binding domain-deficient Munc13-1 mutant 128-Munc13-1 (RIM is also known as RIMS1) was overexpressed in order to prime the vesicles already tethered to the membrane and allow them to proceed to subsequent fusion when Ca^{2+} was present. $[Ca^{2+}]_i$ was then homogeneously increased in the cytosol by uncaging caged Ca^{2+} (NP-EGTA-AM). Under these conditions, the two critical factors that determine the secretory activity are $[Ca^{2+}]_i$ and the number of primed vesicles; ∼25% to 30% of the vesicles were secreted, and neither PMA or α-synuclein had any further effects on the exocytotic activity (Fig. 7D). In addition, there was a dose-dependent increase in exocytosis in cells that were exposed to light for different length of times in order to release different amount of Ca^{2+} (Fig. S5). Therefore, the inhibitory effects of α-synuclein on the PMA-mediated enhancement of secretion (Fig. 6D) is likely to be due to the limited Ca^{2+} concentration in the vicinity of the exocytotic sites. It should be noted that the inhibition of secretion mediated by aggregated α-synuclein remained present. The aggregated α-synuclein would seem therefore to inhibit secretion mainly because of its effects on vesicle priming.

DISCUSSION

The results from this study provide a detailed characterization of the action of α-synuclein in the late steps of exocytosis, including vesicle priming, fusion and dilation of fusion pores. Soluble and aggregated α-synuclein have opposite effects on secretion. Soluble α-synuclein is able to enhance exocytosis by increasing vesicle priming and by bringing about a faster dilation of fusion pore. α-Synuclein and the Rab3A, Munc13 and Munc18 molecules act on the same population of vesicles via different pathways in the regulation of vesicle priming and fusion. Soluble α-synuclein elevates Ca^{2+} release from TG-sensitive Ca^{2+} pools to enhance ATP-evoked fusion, revealing a novel role of α-synuclein in coupling vesicles to specific Ca^{2+} microdomains. In contrast, aggregated α-synuclein, in a Ca^{2+}-independent pathway, brings about an inhibition of vesicle priming, but has no effect on the dilation of fusion pores.

The soluble and aggregated forms of α-synuclein have opposite effects on secretion

The results of the present FRAP study show that overexpressed α-synuclein is present in the monomeric form and lactacystin induces the aggregation α-synuclein. The soluble α-synuclein and aggregated forms of α-synuclein have opposite effects on exocytotic activity (Figs 1–3). Exocytotic activity and the percentage of type 3 secretion were found to be enhanced in α-synuclein-overexpressing PC12 cells (Fig. 1), while at the same time the number of morphological docked vesicles was not affected. These results suggest that soluble α-synuclein enhances the formation of fusion-competent vesicle (vesicle priming) and then promotes exocytosis. The increase in type 3 secretion suggests that α-synuclein also accelerates the dilation of the fusion pore. In contrast, the enhancement of priming, but not the increased rate of fusion pore dilation, was blocked by the lactacystin-induced aggregation of α-synuclein (Fig. 2C). Furthermore, in cells overexpressing

Journal of Cell Science (2018) 131, jcs213017. doi:10.1242/jcs.213017

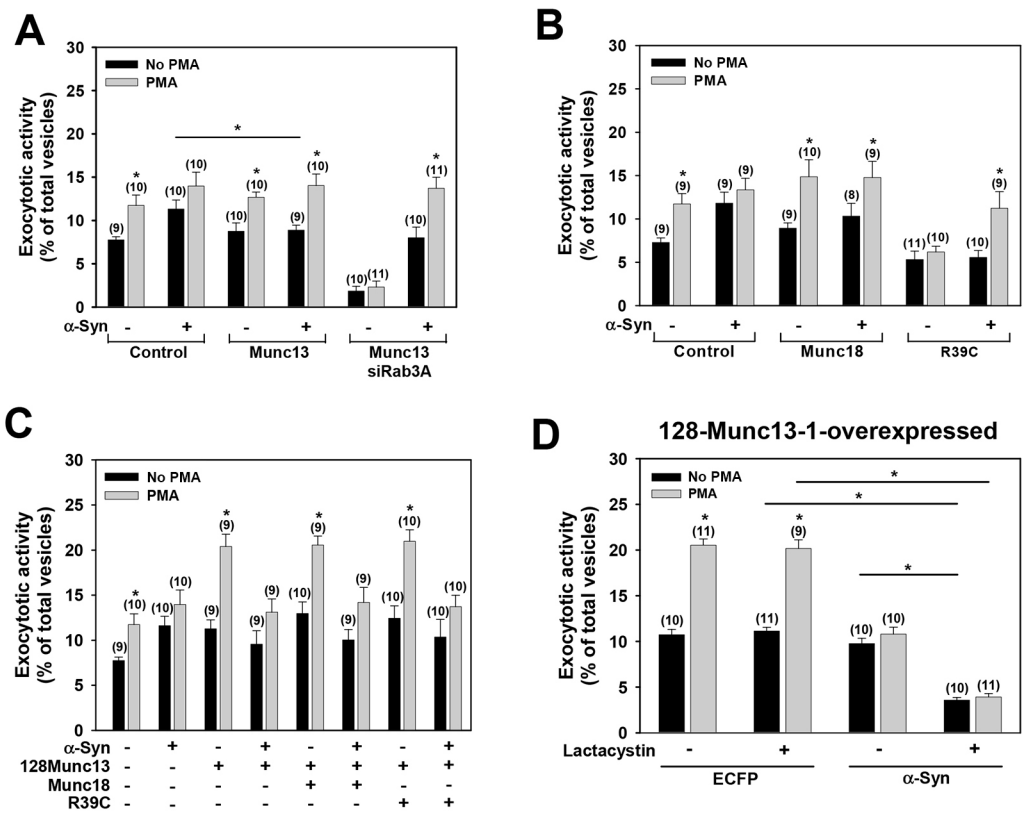

Fig. 6. Effects of α-synuclein on Munc13-1 or Munc18-1-mediated vesicle priming. (A) PC12 cells were transfected with pNPY-EGFP, and pECFP-C1 (Control), pECFP-Munc13-1 (Munc13), or pECFP-Munc13-1 and pSilencer-Rab3A (Munc13 siRab3A), with or without pECFP-α-synuclein (α-Syn + or –) as indicated. (B) PC12 cells were transfected with pNPY-EGFP, and pECFP-C1 (Control), pECFP-Munc18-1 (Munc18) or pECFP-Munc18-1-R39C (R39C) with or without pECFP-α-synuclein (α-Syn + or –) as indicated. (C) PC12 cells were transfected with pNPY-EGFP, and pECFP-C1 (ECFP), pECFP-α-synuclein (α-Syn), pcDNA3.1-128-Munc13-1 (128Munc13), pECFP-Munc18-1 (Munc18) and/or pECFP-Munc18-1-R39C (R39C) as indicated. (D) PC12 cells were transfected with pNPY-EGFP, pcDNA3.1-128-Munc13-1 (128Munc13), and pECFP-C1 (ECFP) or pECFP-α-synuclein (α-Syn) as indicated. After 24 h, the transfected cell were treated with 5 µM lactacystin for 24 h. The transfected cells were pre-treated with 100 nM PMA or control buffer for 10 min. Fluorescence changes in the NPY-EGFP-labeled vesicles upon ATP stimulation were monitored by TIRF microscopy. The exocytotic activities of the cells are shown as percentages of the total NPY-EGFP-labeled vesicles in the evanescent field that were secreted in 2 min. The data shown are mean±s.e.m. from the numbers of the cells indicated in the parenthesis and were obtained from at least three independent transfections, **P*<0.05 vs control without PMA or as indicated (Student's *t*-test; *n*=8–12).

128-Munc13-1, to prime the vesicles already tethered to the membrane and allow exocytosis to be triggered by uncaged Ca^{2+} (Fig. 7D), the inhibitory effects of aggregated α-synuclein induced by lactacystin remained. These results support the hypothesis that the aggregation of α-synuclein actively inhibits exocytosis rather than not supporting an enhancement of exocytosis.

The effects of α-synuclein on exocytosis are controversial. In chromaffin cells (Larsen et al., 2006) and mouse hippocampal neurons (Nemani et al., 2010), overexpression of α-synuclein inhibits secretion. α-Synuclein has been shown to have contradictory effects, promotion or inhibition, on SNARE complex formation in different studies (Burré et al., 2014; DeWitt and Rhoades, 2013). Recent investigation reports that overexpressed α-synuclein and their isomers promote fusion pore dilation but that total exocytosis is reduced in mouse chromaffin cells (Logan et al., 2017). It is possible that the previous contradictory results obtained during various investigations are due to the state of aggregation of α-synuclein under the different experimental conditions used.

α-Synuclein and Rab3A–Munc13-1–Munc18-1 independently regulate vesicle priming and fusion

We have characterized the molecular mechanism involved in the regulation of vesicle priming and fusion pore dilation mediated by α-synuclein. Previously it has been shown that PMA-induced vesicle priming is mediated by Rab3A, Munc13-1 and Munc18-1 (Huang et al., 2011). During the priming process, Rab3A (the GTP-bound form) interacts with Munc13-1 via RIM (see Fig. 8; Dulubova et al., 2005; Huang et al., 2011; Wang et al., 1997). After GTP hydrolysis, Rab3A-GDP dissociates from membrane and this is mediated by its interaction with Munc18-1, which then triggers vesicle fusion (Huang et al., 2011). Furthermore, fusion pore dilation is regulated by the dissociation rate of Rab3A (Lin et al., 2007; Logan et al., 2017).

Previous biochemical investigations support that α-synuclein interacts with Rab3A (Dalfó et al., 2004a,b; Chen et al., 2013). Our results show that α-synuclein has no effect on Rab3A dissociation (Fig. 4). While the activation state of Rab3A regulates vesicle release, fusion pore dilation became faster when α-synuclein is overexpressed; the result being that more than 80% of the exocytosis have the type 3 pattern (Fig. 5C). When the activity of Rab3A was decreased through overexpression of the dominant-negative Rab3A T36N mutant or knockdown of Rab3A, the effects of α-synuclein became dominant with the ATP-evoked exocytosis being enhanced, but with the effect of PMA being diminished (Fig. 5B). Therefore, α-Synuclein and Rab3A regulate exocytosis independently, but, nevertheless, they appear to act on the same population of vesicles.

Overexpression of Munc13-1 and Munc18-1 rescues the enhancement of PMA in α-synuclein-overexpressing cells.

Journal of Cell Science (2018) 131, jcs213017. doi:10.1242/jcs.213017

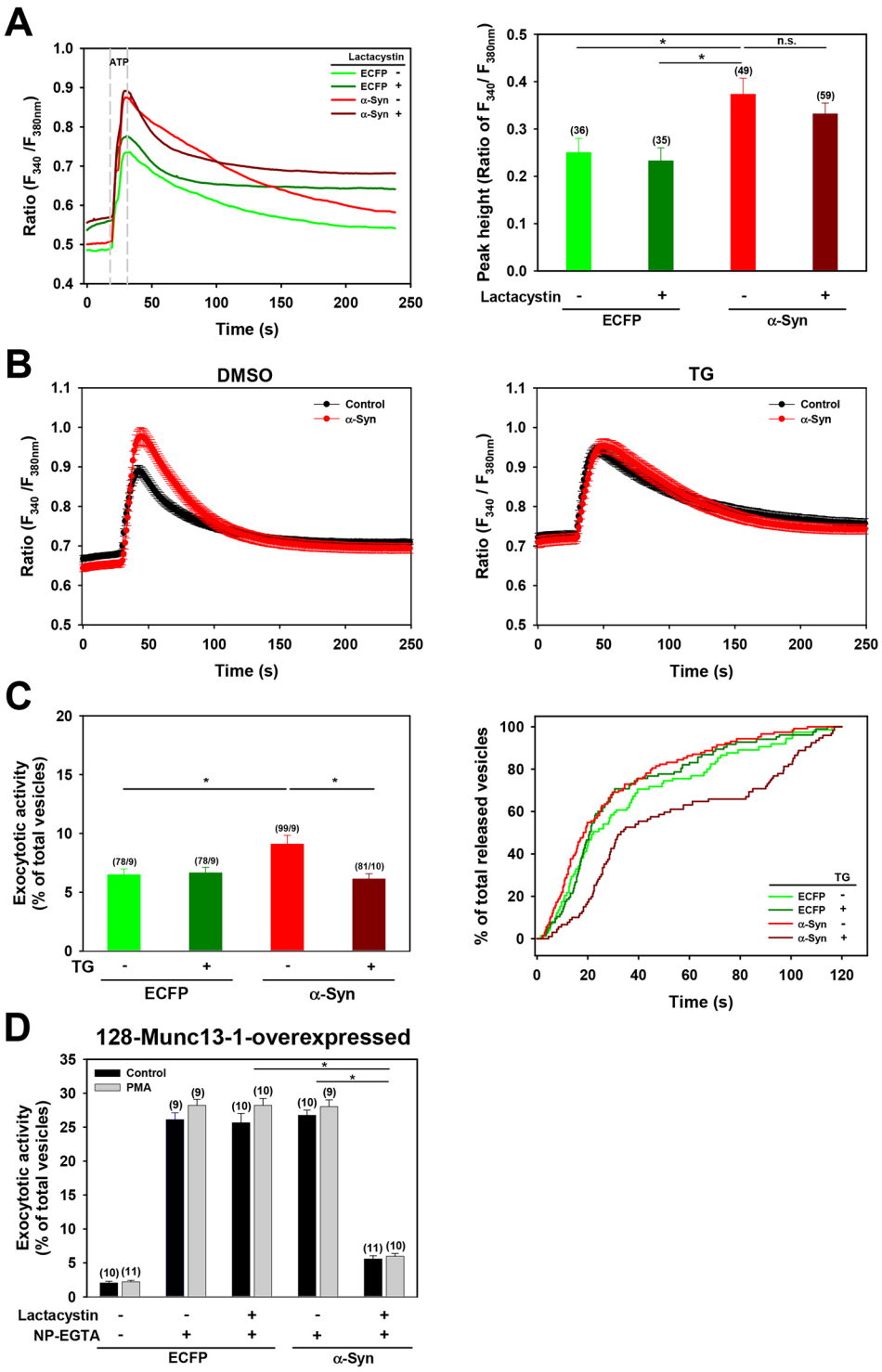

Fig. 7. Effects of α-synuclein on ATP-induced Ca^{2+} response. PC12 cells were co-transfected with pECFP-C1 (ECFP) or pECFP-α-synuclein (α-Syn) for $[Ca^{2+}]_i$ measurements. For exocytosis measurements, pNPY-EGFP and pcDNA3.1-128-Munc13-1 were also expressed as indicated. The transfected cells were pretreated with 5 µM lactacystin for 24 h. (A) Left panel, representative curves showing the changes in $[Ca^{2+}]_i$ upon ATP stimulation. Right panel, averaged peak height of the ATP-induced $[Ca^{2+}]_i$ responses. (B) The transfected cells were pre-treated with DMSO (left panel) or 1 µM TG (right panel) for 10 min. The representative curves show the ATP-induced cytosolic Ca^{2+} changes induced by TG treatment in the control and α-synuclein-overexpressing PC12 cells. (C) Left panel, the exocytotic activities of cells are shown as percentages of total NPY–EGFP-labeled vesicles in the evanescent field that were secreted. Right panel: cumulative NPY-labeled vesicle release events. The time that ATP stimulation started was taken as time 0. (D) The transfected cells were loaded with 50 µM NP-EGTA-AM at 37°C for 45 min. The transfected cells were pre-treated with 100 nM PMA or control buffer for 10 min. Fluorescence changes of the NPY–EGFP-labeled vesicles upon flash photolysis were monitored by TIRF microscopy. The exocytotic activities of the cells are shown as percentages of the total NPY–EGFP-labeled vesicles in the evanescent field that were secreted in 2 min. The data shown are the mean±s.e.m. from the number of cells shown above each column. *P<0.05 vs ECFP-expressing cells (Student's t-test).

In addition, α-synuclein rescues vesicle priming in cells expressing the dominant-negative Munc18-1 mutant, R39C or co-expressing siRNA targeting Rab3A (siRab3A) and Munc13-1 (Fig. 6A,B). Furthermore, overexpression of either the constitutively active Munc13-1 mutant 128-Munc13-1, or α-synuclein brings about an enhancement of secretion; however, co-expression of both molecules had no additive effect (Fig. 6C). Overexpression of 128-Munc13-1 is able to induce more PMA-induced vesicle priming than overexpression of α-synuclein. When α-synuclein is overexpressed, the effect of α-synuclein on priming is dominant. In contrast, when Munc13-1 or Munc18-1, the players in PMA-induced vesicle priming, are overexpressed, the modulation of vesicle priming by the Munc13–Munc18–Rab3A pathway becomes dominant. The step whereby α-synuclein acts in vesicle priming is thus downstream of the interaction of Munc18-1 with syntaxin 1A. These findings support the hypothesis that PMA, mediated by Munc13–Rab3A–Munc18, and α-synuclein act on the same population of vesicles and promote vesicle priming via different pathways.

Aggregated α-synuclein is able to inhibit vesicle secretion and this is independent of the cytosolic Ca^{2+} level (Fig. 7A,B).

Journal of Cell Science (2018) 131, jcs213017. doi:10.1242/jcs.213017

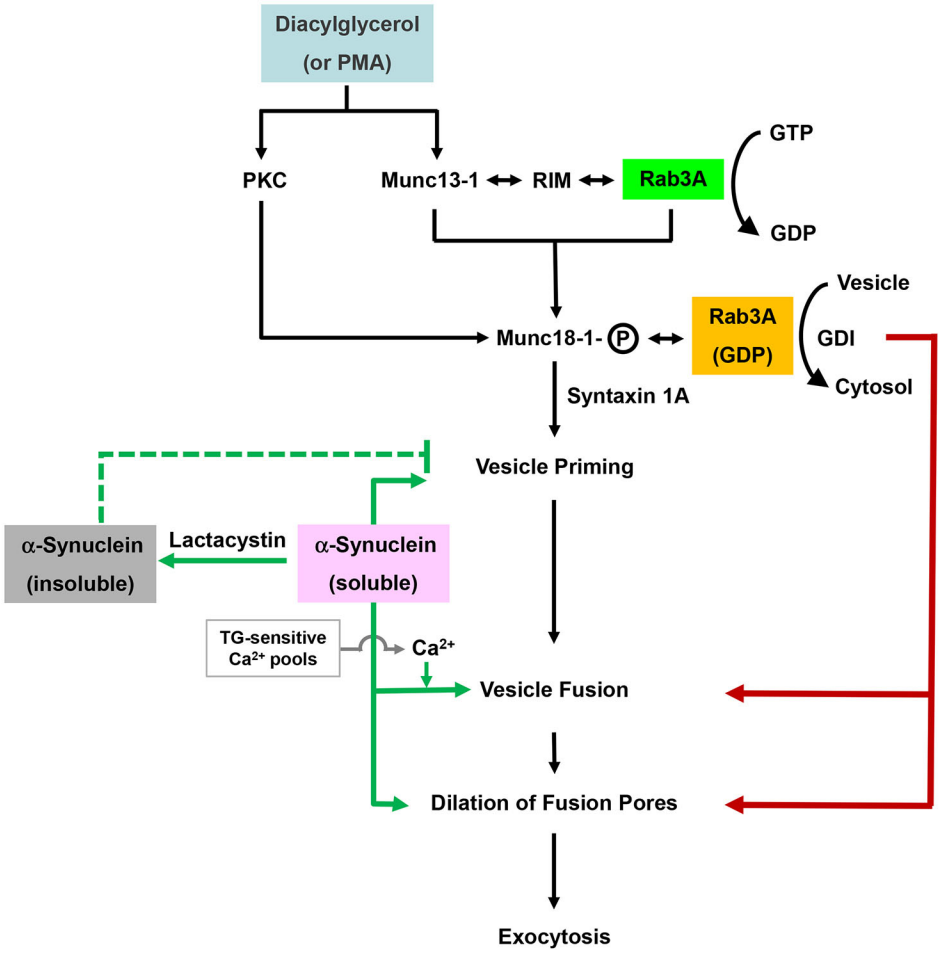

Fig. 8. The molecular mechanism of the late steps exocytosis regulated by α-synuclein. α-Synuclein is involved in the SNARE complex assembly, vesicle priming and fusion. α-Synuclein and Rab3A regulate exocytosis independently, but, nevertheless, they appear to act on the same population of vesicles. When α-synuclein is overexpressed, the effect of α-synuclein on priming is dominant. In contrast, when Munc13-1 or Munc18-1, the players in PMA-induced vesicle priming, are overexpressed, the modulation of vesicle priming by Munc13–Muc18–Rab3A pathway becomes dominant. The step whereby α-synuclein competes in vesicle priming is thus downstream of the interaction of Munc18-1 with syntaxin 1A. α-Synuclein increases the ATP-induced $[Ca^{2+}]_i$ increase by mobilizing the Ca^{2+} released from TG-sensitive Ca^{2+} pools, and this enhances vesicle fusion. Although α-synuclein is also involved in fusion pore dilation, Rab3A remains a gatekeeper for the fusion step.

Furthermore, aggregated α-synuclein appears to interfere with priming, which results in an inhibition of secretion. These findings are compatible with previous findings using a mouse hippocampal neuron model wherein it was found that α-synuclein multimers cluster around vesicles and this results in a restriction of vesicle trafficking that, in turn, attenuates secretion (Wang et al., 2014).

α-Synuclein increases Ca^{2+} release from the TG-sensitive Ca^{2+} pool, which results in enhanced fusion

It is well known that cytosolic Ca^{2+} regulates vesicle docking, priming, fusion and expansion of fusion pores (Man et al., 2015). Our results show a novel effect of α-synuclein on the mobilization of Ca^{2+} from the TG-sensitive Ca^{2+} pools. This release of Ca^{2+} is essential for the enhancement of ATP-induced exocytosis by α-synuclein. The effects of α-synuclein, which shows a lower level of enhancement of ATP-evoked exocytosis than the protein 128-Munc13-1, can be abolished in experiments when there is uncaging of caged $[Ca^{2+}]_i$; this increases $[Ca^{2+}]_i$ homogeneously and triggers the fusion of all vesicles primed by the overexpression of 128-Munc13-1. These findings show that Ca^{2+} from the TG-sensitive pools is required for the effect of α-synuclein on fusion. It is speculated that α-synuclein induces a change in the vesicles during vesicle priming to move them to a position that is closer to the TG-sensitive ER Ca^{2+} pool, so that when the Ca^{2+} is released from this Ca^{2+} pool, the triggering of the subsequent fusion is easier. By way of contrast, aggregated α-synuclein inhibits the exocytosis increase in experiments involving caged Ca^{2+} and cells overexpressing 128-Munc13-1. This suggests that the effects of aggregated α-synuclein is independent of Ca^{2+} (Figs 3B, 7A,B; Man et al., 2015; Tiberiu and Smith, 2006).

Using primary cultured neurons and chromaffin cells, Logan et al. (2017) have recently drawn similar conclusions, namely that α-synuclein facilitates fusion pore dilation and the kinetics of exocytosis. However, their results show that total exocytosis is reduced by overexpression of α-synuclein. The reasons for this discrepancy are not immediately clear. One possibility is that the enhancement effects of α-synuclein requires Ca^{2+} from TG-sensitive Ca^{2+} pool; the high K^+ stimulation used in their study only induces a Ca^{2+} influx via the voltage-gated Ca^{2+} channels and this Ca^{2+} influx is likely to be further away from the α-synuclein-regulated sites than the TG-sensitive Ca^{2+} release.

The molecular mechanism of actions of α-synuclein during the late steps of exocytosis

Based on the results from this study and those of previous researchers, the role of α-synuclein in the priming and dilation of fusion pores, as well as its relationship with Rab3A, is depicted in Fig. 8. It is generally thought that plasma membrane-associated Munc13-1, GTP-Rab3A and RIM form a tripartite complex in the presence of diacylglycerol and Ca^{2+}. Vesicles then dock to the sites of secretion via the tripartite complexes and then interact with phosphorylated Munc18-1 to allow the assembly of the SNARE complex, which allows priming of the vesicles. We have previously found that syntaxin 1A-bound Munc18-1 and GTP hydrolysis are able to bring about the dissociation of Rab3A from vesicles, which allows fusion to occur upon stimulation (Huang et al., 2011).

α-Synuclein and the Munc13-1–Munc18-1–Rab3A pathway, based on the present results, act on different sites of the same population of vesicles during the priming and fusion events of exocytosis. Furthermore, α-synuclein affects fusion by mobilizing Ca^{2+} from the TG-sensitive Ca^{2+} pools, and this possibly causes the dilation of fusion pores. In contrast, aggregated α-synuclein inhibits vesicle priming in a Ca^{2+}-independent manner.

MATERIALS AND METHODS

Plasmids

DNA encoding human α-synuclein with restriction sites at either end (XhoI at the 5′ end and HindIII at the 3′ end) was amplified by PCR from the cDNA of a human sample. The α-synuclein DNA used in this study was a gift from Dr Chang-Jen Huang (Academia Sinica, Taiwan, Republic of China), and was subcloned into pECFP (cyan fluorescence protein)-C1 (Clontech, Palo Alto, CA). The N-terminus of α-synuclein was fused in frame to the C-terminus of ECFP at the XhoI site. Rat Rab3A was subcloned into pECFP-C1 or pEGFP-C1 with the N-terminus fused in frame to the C-terminus of various fluorescence protein genes as described previously (Lin et al., 2007). Rat Munc13-1 and 128-Munc13-1 were subcloned into pECFP-N1 with the C-terminus of Munc13-1 or its truncated mutants fused in frame to the N-terminus of ECFP gene as described previously (Huang et al., 2011). $pEGFP_3$ was provided by Dr Alan M. Lin (Department of Life Sciences, NYMU, Taiwan, Republic of China). pNPY-EGFP was a kind gift from Dr Wolfhard Almers (Vollum Institute, Oregon Health & Science University, OR). The pMunc13-1-EGFP and pMunc13-1-H567K-EGFP mutants were kind gifts from Dr Nils Brose (Max-Planck Institute, Germany). The pECFP-Munc18-1 and pECFP-Munc18-1-R39C mutants were kind gifts from Dr Robert D. Burgoyne (University of Liverpool, UK). pSilencer-Rab3A (Tsuboi and Fukuda, 2006) was a kind gift from Dr Mitsunori Fukuda (Tohoku University, Miyagi, Japan). pNPY-pHluorin was a kind gift from Dr Zhuan Zhou (Peking University, Beijing, China).

Cell culture and transfection

PC12 cells, a rat adrenal pheochromocytoma cell line, were purchased from the American Type Culture Collection (ATCC, Rockville, MD). The PC12 cells were cultured in Dulbecco's modified Eagle's medium (DMEM) containing 10% horse serum (heat-inactivated) and 5% fetal bovine serum (Invitrogen, Carlsbad, CA) (complete medium). For transfection, cells were plated on poly-L-lysine-coated 24 mm coverslips in 35 mm culture dishes at a density of 3×10^5 cells per dish. The PC12 cells were transfected using LipofectAmine-2000® reagent (Invitrogen). Briefly, 1 µg of DNA was diluted into 1 ml serum-free DMEM and then mixed well with 3 µl of the LipofectAmine 2000®. The solution was incubated for at least 20 min before it was added to the cells. Next, the cells were incubated at 37°C in a 10% CO_2 incubator for 1 h, and then 1 ml DMEM containing 20% horse serum and 10% fetal bovine serum was added. After 4 h, the transfection mixture was removed and replaced with fresh complete medium. The transfected cells were used for experiments after 48 h.

Western blot analysis

PC12 cells were co-transfected either pECFP-C1 or pECFP-α-synuclein together with a selection vector, pCI-puro (Promega, Madison, WI). After 24 h, the transfected cells were treated with 5 µg/ml puromycin for 72 h to select for the α-synuclein-expressing cells. Cell lysates was separated by SDS-PAGE and transferred onto a nitrocellulose membrane. After incubation with a monoclonal anti-α-synuclein antibody (1:1000, ab138501, Abcam, Cambridge, MA), the immunoreactive bands of α-synuclein were visualized using the ECL detection system (GE Healthcare, Piscataway, NJ). ECL detection was performed as recommended by the GE Healthcare protocol.

Stimulation of PC12 cells

Transfected PC12 cells that had been grown on coverslips were incubated in control buffer (150 mM NaCl, 5 mM KCl, 1 mM $MgCl_2$, 2.2 mM $CaCl_2$, 5 mM glucose and 10 mM HEPES, pH 7.4). Cells with similar expression levels, as determined by their fluorescence intensity, were selected for stimulation. The cells were stimulated by a pulse of 200 µM ATP for 10 s or 100 nM phorbol-12-myristate-13-acetate (PMA) for 10 min via an ejection micropipette set at a positive pressure of 10 psi (Picospritzer II, Parker Hannifin, Cleveland, OH). The micropipette was pulled from a glass capillary by a micropipette puller (P-97, Sutter, Novato, CA). The tip of the micropipette (external diameter ∼2 µm) was polished using a microforge (MF-83, Narishige, Tokyo, Japan). The ejection micropipette was held by a micromanipulator (MHW-3, Narishige) and positioned at a distance of ∼10 µm away from the cell under study.

TIRF imaging

An objective-type TIRF microscopy system was set up on an inverted microscope (IX-71, Olympus Optical Co., Ltd, Tokyo, Japan). The dual port TIRF/Epi condenser (T.I.L.L. Photonics, Gräfelfing, Germany) was coupled to a multi-line argon laser that could emit at 457–514 nm (45 mW, Melles Griot, Carlsbad, CA) controlled by acousto-optic tunable filters (AOTF) (AA opto-photonic, Orsay Cedex, France) and a xenon lamp (Polychrome IV, T.I.L.L. Photonics). The laser beam was controlled by the TIRF condenser and passed through a high numerical aperture objective (PlanApo 60×, NA 1.45 Oil, Olympus Optical Co., Ltd) to produce an evanescent field at the cell–coverslip interface. Both TIRF and epi-fluorescence images were acquired via an electron multiplying CCD camera (pixel size 8×8 µm, iXon 885, Andor Technology, UK) controlled by a commercial software (TILLvisION 4.0, T.I.L.L. Photonics); this also controlled other related hardware including the shutters of the laser and Xenon lamp. The TIRF images were acquired at 300 ms/frame unless otherwise indicated.

Tracking of individual secretory vesicles

The fluorescence of a single vesicle in the TIRF images was analyzed using commercial software (DiaTrack 3.0, Semasopht, Chavannes, Switzerland) as previously described (Lin et al., 2007). Single vesicles were automatically tracked by monitoring the position of the pixel with the highest fluorescence intensity. The fluorescent spots in the first frame of the TIRF images were initially identified by the tracking system. Next, the spots that had been identified were confirmed manually before automatic tracking was allowed to proceed. After tracking, the vesicles with fluorescence changes between the first frame and the last frame of images were identified. Vesicles that disappeared were taken as candidates that had undergone exocytosis, and their fluorescence changes were further analyzed. The fluorescence (F) was normalized relative to the first frame before stimulation (F_0).

Fluorescence recovery after photobleaching

FRAP was performed using a laser scanning confocal fluorescence microscope (IX81-based FV1000, Olympus, Japan). The filter sets used for excitation and emission light were 405 and 477 nm for ECFP, 488 and 509 nm for EGFP, and 515 and 537 nm for EYFP, respectively. Areas of interest in the cells that were expressing fluorescence proteins were selected and bleached with a 405 nm laser (25 mW, Melles Griot, Carlsbad, CA) for 500 ms. Time-lapse images of fluorescence recovery were acquired at 65 ms/frame for 600 frames. Intensity changes within the bleached area and the unbleached area, both of which were obtained from the time-lapsed micrographs, were measured. The FRAP curve of the bleached area was corrected against that of the unbleached area (Wu et al., 2006). The corrected plot was fitted to an exponential decay model in order to calculate the recovery half-life ($t_{1/2}$) of the various fluorescence proteins.

Ca^{2+} imaging

Transfected PC12 cells were loading with 10 µM fura-2-AM and incubated at 37°C for 45 min in control buffer (150 mM NaCl, 5 mM KCl, 1 mM $MgCl_2$, 2.2 mM $CaCl_2$, 5 mM glucose, and 10 mM HEPES, pH 7.4). The fura-2 fluorescence ratio obtained by 340 nm and 380 nm excitation was monitored by an inverted microscope (IX-71, Olympus Optical Co., Ltd, Tokyo, Japan) coupled with a Xenon lamp monochromator (Polychrome IV, T.I.L.L. Photonics) and a CCD camera (pixel size 6.7×6.7 µm, 1300YHS,

Princeton Instruments, Princeton, NJ) controlled by a commercial software (MetaFluor, Molecular Device, Sunnyvale, CA).

Photolysis of caged Ca^{2+}

Transfected PC12 cells were incubated with 50 µM Nitrophenyl-EGTA (NP-EGTA) AM at 37°C for 45 min in control buffer (150 mM NaCl, 5 mM KCl, 1 mM $MgCl_2$, 2.2 mM $CaCl_2$, 5 mM glucose, and 10 mM HEPES, pH 7.4). The cells were then washed twice to remove extracellular NP-EGTA AM. Ca^{2+} uncaging was carried out using a high-energy ultraviolet light flash system (JML-C2, Rapp Opto-Electronic, Germany) to apply a pulse of UV light (375 V), for 50–200 ms as indicated (Fig. S2), which released the caged Ca^{2+}, which, in turn, triggers exocytosis (Xu, et al., 1998).

Acknowledgements
We thank Dr Yeh-Shiu Chu (Brain Research Center, National Yang-Ming University) for his help in acquiring TIRF images.

Competing interests
The authors declare no competing or financial interests.

Author contributions
L.-S.K. and C.-C.L. designed and supervised the study and wrote the manuscript. C.-C.H. designed and performed the experiments and wrote the manuscript. T.-Y.C. and T.-Y.L. constructed the fluorescence protein-tagged α-synuclein and discovered the effect of α-synuclein on fusion pore dilation. H.-J.H. measured the solubility of α-synuclein in PC12 cells by FRAP.

Author contributions
Conceptualization: C.-C.H., C.-C.L., L.-S.K.; Methodology: T.-Y.C.; Formal analysis: C.-C.H.; Investigation: C.C.H., T.-Y.C., T.-Y.L., H.-J.H.; Writing - original draft: C.-C.H.; Writing - review & editing: C.-C.L., L.-S.K.; Visualization: C.-C.H.; Supervision: C.-C.L., L.-S.K.; Project administration: L.-S.K.; Funding acquisition: C.-C.L., L.-S.K.

Funding
The study was supported by grants from Ministry of Science and Technology, Taiwan, Republic of China (to L.-S.K., MOST102-2311-B-010-007-MY3, MOST102-2811-B-010-049, MOST103-2811-B-010-035, MOST104-2811-B-010-031), and the Aim for the Top University Plan and the Featured Areas Research Center Program within the framework of the Higher Education Sprout Project, Ministry of Education, Republic of China.

Supplementary information
Supplementary information available online at
http://jcs.biologists.org/lookup/doi/10.1242/jcs.213017.supplemental

References

Abeliovich, A., Schmitz, Y., Fariñas, I., Choi-Lundberg, D., Ho, W.-H., Castillo, P. E., Shinsky, N., Verdugo, J. M. G., Armanini, M., Ryan, A. et al. (2000). Mice lacking alpha-synuclein display functional deficits in the nigrostriatal dopamine system. *Neuron* **25**, 239-252.

Burré, J., Sharma, M. and Südhof, T. C. (2014). α-Synuclein assembles into higher-order multimers upon membrane binding to promote SNARE complex formation. *Proc. Natl. Acad. Sci. USA* **111**, E4274-E4283.

Cabin, D. E., Shimazu, K., Murphy, D., Cole, N. B., Gottschalk, W., McIlwain, K. L., Orrison, B., Chen, A., Ellis, C. E., Paylor, R. et al. (2002). Synaptic vesicle depletion correlates with attenuated synaptic responses to prolonged repetitive stimulation in mice lacking alpha-synuclein. *J. Neurosci.* **22**, 8797-8807.

Chandra, S., Gallardo, G., Fernández-Chacón, R., Schlüter, O. M. and Südhof, T. C. (2005). Alpha-synuclein cooperates with CSPalpha in preventing neurodegeneration. *Cell* **123**, 383-396.

Chen, R. H. C., Wislet-Gendebien, S., Samuel, F., Visanji, N. P., Zhang, G., Marsilio, D., Langman, T., Fraser, P. E. and Tandon, A. (2013). α-Synuclein membrane association is regulated by the Rab3a recycling machinery and presynaptic activity. *J. Biol. Chem.* **288**, 7438-7449.

Dalfó, E., Barrachina, M., Rosa, J. L., Ambrosio, S. and Ferrer, I. (2004a). Abnormal alpha-synuclein interactions with rab3a and rabphilin in diffuse Lewy body disease. *Neurobiol. Dis.* **16**, 92-97.

Dalfó, E., Gómez-Isla, T., Rosa, J. L., Bodelón, M. N., Tejedor, M. C., Barrachina, M., Ambrosio, S. and Ferrer, I. (2004b). Abnormal alpha-synuclein interactions with Rab proteins in alpha-synuclein A30P transgenic mice. *J. Neuropathol. Exp. Neurol.* **63**, 302-313.

DeWitt, D. C. and Rhoades, E. (2013). α-Synuclein can inhibit SNARE-mediated vesicle fusion through direct interactions with lipid bilayers. *Biochemistry* **52**, 2385-2387.

Dulubova, I., Lou, X., Lu, J., Huryeva, I., Alam, A., Schneggenburger, R., Südhof, T. C. and Rizo, J. (2005). A Munc13/RIM/Rab3 tripartite complex: from priming to plasticity? *EMBO J.* **24**, 2839-2850.

Fortin, D. L., Troyer, M. D., Nakamura, K., Kubo, S., Anthony, M. D. and Edwards, R. H. (2004). Lipid rafts mediate the synaptic localization of alpha-synuclein. *J. Neurosci.* **24**, 6715-6723.

Fortin, D. L., Nemani, V. M., Voglmaier, S. M., Anthony, M. D., Ryan, T. A. and Edwards, R. H. (2005). Neural activity controls the synaptic accumulation of α-synuclein. *J. Neurosci.* **25**, 10913-10921.

Fisher, R. J., Pevsner, J. and Burgoyne, R. D. (2001). Control of fusion pore dynamics during exocytosis by Munc18. *Science* **291**, 875-878.

Gourine, A. V., Wood, J. D. and Burnstock, G. (2009). Purinergic signalling in autonomic control. *Trends Neurosci.* **32**, 241-248.

Hettiarachchi, N. T., Parker, A., Dallas, M. L., Pennington, K., Hung, C.-C., Pearson, H. A., Boyle, J. P., Robinson, P. and Peers, C. (2009). alpha-Synuclein modulation of Ca^{2+} signaling in human neuroblastoma (SH-SY5Y) cells. *J. Neurochem.* **111**, 1192-1201.

Huang, C.-C., Yang, D.-M., Lin, C.-C. and Kao, L.-S. (2011). Involvement of Rab3A in vesicle priming during exocytosis: interaction with Munc13-1 and Munc18-1. *Traffic* **12**, 1356-1370.

Ihara, M., Yamasaki, N., Hagiwara, A., Tanigaki, A., Kitano, A., Hikawa, R., Tomimoto, H., Noda, M., Takanashi, M., Mori, H. et al. (2007). Sept4, a component of presynaptic scaffold and Lewy bodies, is required for the suppression of alpha-synuclein neurotoxicity. *Neuron* **53**, 519-533.

Kahle, P. J., Neumann, M., Ozmen, L., Müller, V., Jacobsen, H., Schindzielorz, A., Okochi, M., Leimer, U., van Der Putten, H., Probst, A. et al. (2000). Subcellular localization of wild-type and Parkinson's disease-associated mutant alpha-synuclein in human and transgenic mouse brain. *J. Neurosci.* **20**, 6365-6373.

Kumar, M., Mommer, M. S. and Sourjik, V. (2010). Mobility of cytoplasmic, membrane, and DNA-binding proteins in *Escherichia coli*. *Biophys J.* **98**, 552-559.

Larsen, K. E., Schmitz, Y., Troyer, M. D., Mosharov, E., Dietrich, P., Quazi, A. Z., Savalle, M., Nemani, V., Chaudhry, F. A., Edwards, R. H. et al. (2006). Alpha-synuclein overexpression in PC12 and chromaffin cells impairs catecholamine release by interfering with a late step in exocytosis. *J. Neurosci.* **26**, 11915-11922.

Leenders, A. G. M., Lopes da Silva, F. H., Ghijsen, W. E. J. M. and Verhage, M. (2001). Rab3a is involved in transport of synaptic vesicles to the active zone in mouse brain nerve terminals. *Mol. Biol. Cell* **12**, 3095-3102.

Lin, C.-C., Huang, C.-C., Lin, K.-H., Cheng, K.-H., Yang, D.-M., Tsai, Y.-S., Ong, R.-Y., Huang, Y.-N. and Kao, L.-S. (2007). Visualization of Rab3A dissociation during exocytosis: a study by total internal reflection microscopy. *J. Cell Physiol.* **211**, 316-326.

Logan, T., Bendor, J., Toupin, C., Thorn, K. and Edwards, R. H. (2017). α-Synuclein promotes dilation of the exocytotic fusion pore. *Nat. Neurosci.* **20**, 681-689.

Lu, J., Machius, M., Dulubova, I., Dai, H., Südhof, T. C., Tomchick, D. R., Rizo, J. (2006). Structural basis for a Munc13-1 homodimer to Munc13-1/RIM heterodimer switch. *PLoS Biol.* **4**, e192.

Man, K. N. M., Imig, C., Walter, A. M., Pinheiro, P. S., Stevens, D. R., Rettig, J., Sørensen, J. B., Cooper, B. H., Nils Brose, N. and Wojcik, S. M. (2015). Identification of a Munc13-sensitive step in chromaffin cell large dense-core vesicle exocytosis. *eLife* **4**, e10635.

Maroteaux, L., Campanelli, J. T. and Scheller, R. H. (1988). Synuclein: a neuron-specific protein localized to the nucleus and presynaptic nerve terminal. *J. Neurosci.* **8**, 2804-2815.

Masliah, E., Rockenstein, E., Veinbergs, I., Mallory, M., Hashimoto, M., Takeda, A., Sagara, Y., Sisk, A. and Mucke, L. (2000). Dopaminergic loss and inclusion body formation in alpha-synuclein mice: implications for neurodegenerative disorders. *Science* **287**, 1265-1269.

Murphy, D. D., Rueter, S. M., Trojanowski, J. Q. and Lee, V. M.-Y. (2000). Synucleins are developmentally expressed, and alpha-synuclein regulates the size of the presynaptic vesicular pool in primary hippocampal neurons. *J. Neurosci.* **20**, 3214-3220.

Narhi, L., Wood, S. J., Steavenson, S., Jiang, Y., Wu, G. M., Anafi, D., Kaufman, S. A., Martin, F., Sitney, K., Denis, P. et al. (1999). Both familial Parkinson's disease mutations accelerate alpha-synuclein aggregation. *J. Biol. Chem.* **274**, 9843-9846.

Nemani, V. M., Lu, W., Berge, V., Nakamura, K., Onoa, B., Lee, M. K., Chaudhry, F. A., Nicoll, R. A. and Edwards, R. H. (2010). Increased expression of alpha-synuclein reduces neurotransmitter release by inhibiting synaptic vesicle reclustering after endocytosis. *Neuron* **65**, 66-79.

Outeiro, T. F., Putcha, P., Tetzlaff, J. E., Spoelgen, R., Koker, M., Carvalho, F., Hyman, B. T. and McLean, P. J. (2008). Formation of toxic oligomeric alpha-synuclein species in living cells. *PLoS ONE* **3**, e1867.

Rhee, J.-S., Betz, A., Pyott, S., Reim, K., Varoqueaux, F., Augustin, I., Hesse, D., Südhof, T. C., Takahashi, M., Rosenmund, C. et al. (2002). β-phorbol ester- and diacylglycerol-induced augmentation of transmitter release is mediated by Munc13s and not by PKCs. *Cell* **108**, 121-133.

Reits, E. A. and Neefjes, J. J. (2001). From fixed to FRAP: measuring protein mobility and activity in living cells. *Nat. Cell Biol.* **3**, E145-147.

Rideout, H. J., Larsen, K. E., Sulzer, D. and Stefanis, L. (2001). Proteasomal inhibition leads to formation of ubiquitin/alpha-synuclein-immunoreactive inclusions in PC12 cells. *J. Neurochem.* **78**, 899-908.

Sakisaka, T., Meerlo, T., Matteson, J., Plutner, H. and Balch, W. E. (2002). Rab-alphaGDI activity is regulated by a Hsp90 chaperone complex. *EMBO J.* **21**, 6125-6135.

Spillantini, M. G., Crowther, R. A., Jakes, R., Hasegawa, M. and Goedert, M. (1998). Alpha-Synuclein in filamentous inclusions of Lewy bodies from Parkinson's disease and dementia with lewy bodies. *Proc. Natl. Acad. Sci. USA* **95**, 6469-6473.

Spinelli, K. J., Taylor, J. K., Osterberg, V. R., Churchill, M. J., Pollock, E., Moore, C., Meshul, C. K. and Unni, V. K. (2014). Presynaptic alpha-synuclein aggregation in a mouse model of Parkinson's disease. *J. Neurosci.* **34**, 2037-2050.

Tiberiu, F. and Smith, C. (2006). Physiological stimulation regulates the exocytic mode through calcium activation of protein kinase C in mouse chromaffin cells. *Biochem. J.* **399**, 111-119.

Tsuboi, T. and Fukuda, M. (2006). Rab3A and Rab27A cooperatively regulate the docking step of dense-core vesicle exocytosis in PC12 cells. *J. Cell Sci.* **119**, 2196-2203.

Wang, Y., Okamoto, M., Schmitz, F., Hofmann, K. and Südhof, T. C. (1997). Rim is a putative Rab3 effector in regulating synaptic-vesicle fusion. *Nature* **388**, 593-598.

Wang, X., Thiagarajan, R., Wang, Q., Tewolde, T., Rich, M. M. and Engisch, K. L. (2008). Regulation of quantal shape by Rab3A: evidence for a fusion pore-dependent mechanism. *J. Physiol.* **586**, 3949-3962.

Wang, L., Das, U., Scott, D. A., Tang, Y., McLean, P. J. and Roy, S. (2014). α-synuclein multimers cluster synaptic vesicles and attenuate recycling. *Curr. Biol.* **24**, 2319-2326.

Wu, Y.-X., Masison, D. C., Eisenberg, E. and Greene, L. E. (2006). Application of photobleaching for measuring diffusion of prion proteins in cytosol of yeast cells. *Methods* **39**, 43-49.

Xu, T., Binz, T., Niemann, H. and Neher, E. (1998). Multiple kinetic components of exocytosis distinguished by neurotoxin sensitivity. *Nat. Neurosci.* **1**, 192-200.

Zenisek, D., Steyer, J. A. and Almers, W. (2000). Transport, capture and exocytosis of single synaptic vesicles at active zones. *Nature* **406**, 849-854.